SPR platform based on image acquisition for HER2 antigen detection

2017 Nanotechnology 28 045206

(http://iopscience.iop.org/0957-4484/28/4/045206)

IOP Publishing Nanotechnology

Nanotechnology **28** (2017) 045206 (7pp) doi:10.1088/1361-6528/28/4/045206

SPR platform based on image acquisition for HER2 antigen detection

Johny P Monteiro[1,5,6], Sheila M Predabon[1], Elton G Bonafé[2], Alessandro F Martins[2,3], Alexandre G Brolo[4], Eduardo Radovanovic[1] and Emerson M Girotto[1]

[1] Materials Chemistry and Sensors Laboratories, Department of Chemistry, State University of Maringá, Colombo Avenue 5790, 87020-900, Maringá, PR, Brazil
[2] Department of Chemistry, Federal University of Technology—UTFPR-AP, 86812-460, Apucarana, PR, Brazil
[3] Postgraduate in Materials Science & Engineering, Federal University of Technology—UTFPR-LD, 86036-370 Londrina, PR, Brazil
[4] Department of Chemistry, University of Victoria, PO Box 3065, V8W 3V6 Victoria, BC, Canada

E-mail: johnymonteiro@utfpr.edu.br.

Received 11 August 2016, revised 24 October 2016
Accepted for publication 7 November 2016
Published 20 December 2016

Abstract

HER2 antigen is a marker used for breast cancer diagnosis and prevention. Its determination has great importance since breast cancer is one of the most insidious types of cancer in women. HER2 antigen assessment in human serum is traditionally achieved by enzyme-linked immunosorbent assay (ELISA method), but it has some disadvantages, such as suppressing the thermodynamic–kinetic studies regarding the antibody–antigen interaction, and the use of labeled molecules that can promote false positive responses. Biosensors based on surface plasmon resonance (SPR) are sensitive optical techniques widely applied on bioassays. The plasmonic devices do not operate with labeled molecules, overcoming conventional immunoassay limitations, and enabling a direct detection of target analytes. In this way, a new SPR biosensor to assess HER2 antigen has been proposed, using nanohole arrays on a gold thin film by signal transduction of transmitted light measurements from array image acquisitions. These metallic nanostructures may couple the light directly on surface plasmons using a simple collinear arrangement. The proposed device reached an average sensitivity for refractive index (RI) variation on a metal surface of 4146 intensity units/RIU (RIU = RI units). The device feasibility on biomolecular assessment was evaluated. For this, 3 ng ml^{-1} known HER2 antigen concentration was efficiently flowed (using a microfluidic system) and detected from aqueous solutions. This outcome shows that the device may be a powerful apparatus for bioassays, particularly toward breast cancer diagnosis and prognosis.

Keywords: biosensor, surface plasmon resonance, SPR, HER2 antigen, nanohole array

(Some figures may appear in colour only in the online journal)

1. Introduction

Cancer markers are chemical substances found in abnormal concentrations in urine, blood, and feces, or even in body tissues, of people with cancer. Both sick and healthy cells often produce substances used as cancer markers. Thus, abnormal marker levels can be used to indicate cancer presence, as well as to predict the disease behavior or response to

[5] Present Addresses. Department of Chemistry, Federal University of Technology—UTFPR-AP, Marcílio Dias Street, 635, Post Code 86812-460, Apucarana, PR, Brazil and Postgraduate in Materials Science & Engineering, Federal University of Technology—UTFPR-LD, 86036-370 Londrina, PR, Brazil.
[6] Author to whom any correspondence should be addressed.

treatment. In this sense, it will be possible to assess the chance of patient recovery against cancer, allowing an appropriate treatment, and even to find cancer in seemingly healthy people [1]. Currently, cancer antigens are the most widely used markers [2].

Human epidermal receptor 2 (HER2) oncogene protein is a transmembrane glycoprotein of the epidermal growth factor receptor family. This gene is found at a low concentration in healthy epithelial tissues, including mammary duct epithelium. However, gene amplification combined with overexpression of signaling protein (antigen) has been found at 15%–20% and at 20%–40% in individuals with primary and invasive breast cancer, respectively [3]. HER2 antigen assessment is important because it can be used in breast cancer diagnostics and prognostics [4, 5]. Healthy individuals show up to 2–15 ng ml^{-1} HER2 in blood, while patients with breast cancer have 15–75 ng ml^{-1} levels [6].

HER2 screening in tissues is usually performed by immunohistochemistry (IHC) [5, 7, 8], which is a good choice to assess HER2 status because such a technique occurs with low reagent consumption. However, the IHC technique has shown less accuracy [9], therefore the fluorescence *in situ* hybridization (FISH) technique has also been employed [5, 8, 10, 11]. FISH is a 'gold standard' testing, but demands a lot of time, and is consequently a more expensive process compared to IHC [5, 8]. Electrochemical biosensors have been recently reported to achieve the HER2 assessment, but in human serum samples [12, 13]. Nevertheless, enzyme-linked immunosorbent assay (ELISA) is traditionally carried out to assess HER2 in blood [14–18], and such a conventional immunological technique is mostly used for HER2 evaluation. However, this immunoassay takes place using labeled molecules, such as fluorophores, phosphors, enzymes or even dial-radioactive. Molecular labeling can often change the antigen recognition activity towards elements, leading to false-negative or positive outcomes because protein aggregation may occur [19]. Furthermore, the antigen detection by ELISA assay is based on an obtained response due to the formation of a complex between a labeled antibody and an antigen, previously immobilized on a capture antibody (sandwich assay). Thus, the ELISA assay cannot evaluate the kinetic and thermodynamic studies concerning antigen–antibody interaction. Biosensors based on the surface plasmon resonance (SPR) effect are well-established analytical techniques which show some interesting features, such as molecular labeling absence (label-free devices), real-time information, high sensitivity, and the possibility of a direct detection [20]. In addition, these devices have already been used in immunoassay analyses to assess the HER2 marker [21].

Surface plasmons (SPs) are light waves trapped on metal–dielectric surfaces due to their resonant interactions with electrons of the metal conduction band [22]. SPs were firstly reported by Fano [23] to explain the diffracted light spectrum anomalies caused by metallic diffraction gratings, previously reported by Wood [24]. In 1968, Otto [25] and Kretschmann [26] independently produced methods for surface plasmon excitation. Since then, the attenuated total internal reflectance configuration, using thin metal films coupled to a prism (proposed by Kretschmann) has been employed in many commercial affinity biosensors [27]. The plasmonic waves are much more sensitive to refractive index (RI) changes in the surrounding environment above the metal surface. Thus, binding events between a recognition element (immobilized on metal film) and target molecules (in the dielectric) may be optically monitored [27]. This is the main feature exploited to build plasmonic biosensors.

Several researchers have recently shown that SPs can be generated easily from nanohole arrays built in noble metal thin films which have been applied to obtain label-free affinity biomolecular sensors [22, 28–30]. Biosensors based on subwavelength nanohole arrays show some advantages with regards to those traditional devices used by Kretschmann. Such biosensors are composed of an easier experimental setup that operates from a collinear transmission mode, allowing better potential for miniaturization [28, 29]. These devices exploit the extraordinary optical transmission (EOT) phenomenon for subwavelength nanohole arrays manufactured in gold and silver thin films [31, 32]. Under EOT, a greater intensity of transmitted light is observed through nanohole arrays than that predicted by the classical diffraction laws. This nanostructured metal property was associated with the presence of SPs, so the characteristics of the transmitted light are dependent on RI changes on the metal surface. Therefore, transmission measurements can be used to monitor binding events. Many studies show that biological substance detection can be performed from SPR biosensors based on nanohole arrays, monitoring the shifts on transmission maximum wavelength [22, 29, 30]. However, the signal transduction using transmitted light intensity measurements have been explored in a few works [33–35]. The monitoring of several binding events on the same platform is the main advantage of the approach based on intensity investigation.

In this paper, we propose a new and sensitive label-free SPR biosensor based on subwavelength nanohole arrays integrated to a microfluidic system, and applied to assess lesser HER2 antigen amounts from an aqueous solution. Analyses were based on the investigation of transmitted light intensity through the nanostructures. This method has not been exploited to assess such a cancer marker yet.

2. Methods

2.1. Materials

Glass slides 2.5 × 2.5 × 0.1 cm covered with chromium films (5 nm thick), and afterwards gold (100 nm thick), were used to obtain substrates containing nanohole arrays. To characterize the substrate sensitivity, aqueous solutions of D-(+)-glucose (Sigma, 99.5%) were used. For the gold surface modification, cysteamine (Aldrich, 95%), sulfo-NHS-biotin (Sigma-Aldrich, 90%), and streptavidin (Sigma, 65%) were used. A biotinylated specific antibody against HER2 antigen (95%), as well as the HER2 antigen (70%), were obtained from Invitrogen. To prepare the microfluidic system,

a kit purchased from Sylgard® 184 was used which contained elastomer polydimethylsiloxane (PDMS) and a curing agent; a photoresist (SU-8® 50) and SU-8 developer were purchased from Microchem. To prepare the phosphate-buffered saline (PBS), NaCl (95.5%) and NaH_2PO_4 (98.0%) solution purchased from Sigma was used; KCl (99.0%) and Na_2HPO_4 (99.0%) were obtained from Sigma-Aldrich. 'Antigen solution' (AS) was prepared by adding Triton X-100, cold fish skin gelatin and bovine serum albumin (BSA, 96%), all acquired from Sigma. H_2SO_4 (FMaia, 95.0%) and H_2O_2 (Anidrol, 35.0%) were used to obtain the solution for metallic substrate cleaning.

2.2. Nanohole arrays obtainment

Nanohole arrays were obtained by focused ion beam (FIB, FEI 235 dual-beam), using a gallium ion source. The ion beam was set to 30 keV with 1.6 nm μs^{-1} milling rate and 300 nA beam current. In this case, four arrays were obtained. The substrate was characterized by scanning electron microscopy (SEM, Shimadzu Superscan SSX-550).

2.3. Microfluidic system

Glass slides were cleaned with 30 ml of 'piranha solution' (3:1 H_2SO_4:H_2O_2 (v/v)) to remove organic residues and promote better photoresist adhesion to the slide. SU-8 photoresist film was obtained by a spin coater (Spincoating Systems, G3P-8) on the cleaned substrate. For this, *ca.* 0.5 g SU-8 was dripped onto the slide center and a proper rotation schedule was performed in order to obtain a homogeneous photoresist film of *ca.* 50 μm thickness. Initially, a rotation of 500 rpm was achieved at a 100 rpm s^{-1} rate (starting from rest), and then held for 10 s. Subsequently, the rotation was increased to 2000 rpm (at a 400 rpm s^{-1} rate) and held for 25 s. The total program lasted *ca.* 45 s.

After that, the substrate containing photoresist film was placed on a heating plate at 60 °C for 6 min, and then heated at 95 °C for 25 min (solvent removal). Immediately after heating, a photomask (a PET sheet containing the print of the microchannels design) was placed on the substrate. The assembly was left in a light collimator (Tamarack Scientific, 2110CP), where it was exposed to UV light for 17.5 s. Then, the substrate with the photograved microchannel pattern was again heated at 60 °C for 1 min, and then heated at 95 °C for 5 min. For the microchannels revelation, the glass slide containing the photograved photoresist was immersed in an SU-8 developer solution (ethyl lactate-based solution, which solubilizes the area not exposed to UV light) with manual stirring at room temperature until complete solubilization occurred. After this treatment, the mold was obtained.

For the microchannel fabrication on PDMS, *ca.* 20 g of 10:1 (w/w) PDMS/curing agent solution was dispensed on the obtained mold, which was positioned inside the petri dish. The assembly was taken to cure on a heating plate at 90 °C for 2 h. Finally, the solid and flexible elastomer was removed from the mold and the system was ready. The experimental scheme for obtaining microchannels in PDMS (by soft lithography) can be found in the supplementary data.

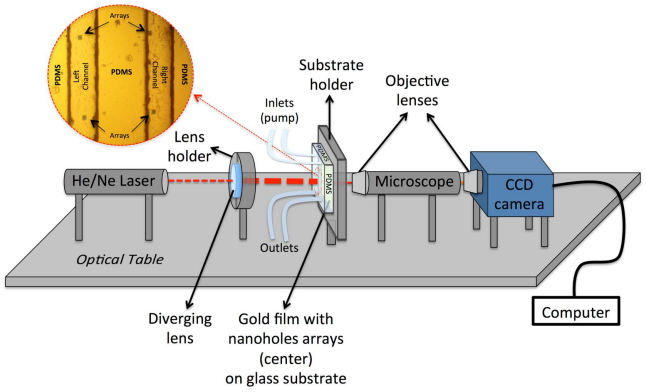

Figure 1. Experimental setup used to monitor the light intensity transmitted by the nanohole arrays. Top inset: photographic image, showing the arrays aligned with the microchannels manufactured on the PDMS piece.

2.4. Optical measurements: image acquisition

The microchannels manufactured on the PDMS were perfectly aligned with the nanohole arrays using a trinocular optical microscope (Quimis, Q738MIT) equipped with a 10x objective lens to view the arrays. A photographic image showing the arrays aligned with the microchannels is depicted in figure 1 (top inset). After alignment, the assembly was fixed to an aluminum substrate holder. Tubes were connected to the PDMS piece (inlets and outlets) to perform the solution flow into the channel using a syringe pump (Harvard Apparatus 11 Plus).

To monitor the intensity of the light transmitted through the arrays, the arrangement shown schematically in figure 1 was used. The light source used for plasmon excitation was a HeNe laser (Melles Griot CVI, 23-LHP-991-230) which emits at 632.8 nm. The light beam was spread uniformly over the substrate via a biconvex lens. The transmitted light was then collected by a measuring microscope (Precision, telescope type) equipped with a 10x objective lens that was positioned on the opposite side to the light incidence. The light was then directed to a CCD digital camera (Roper Scientific, coolsnapk4), equipped with a 10x objective lens, which collected array images. From the images, the transmitted light intensities were obtained using the software Image J considering the entire array area. The experimental system was fully assembled on an optical table (Melles Griot).

2.5. Sensitivity characterization

To evaluate the plasmonic substrate response concerning RI variation on a metal surface, aqueous glucose solutions were performed at 2.0, 6.0, 10.0, 14.0, 18.0, 22.0, 26.0 and 30.0 g/100 ml. RIs of each solution were determined using a portable digital refractometer (Atago, PAL-RI 3850). The solutions were flowed on the arrays using the experimental setup shown in figure 1. A 2.00 ml h^{-1} flow was used, and, after it stopped, 50 subsequent images were recorded for each nanostructure

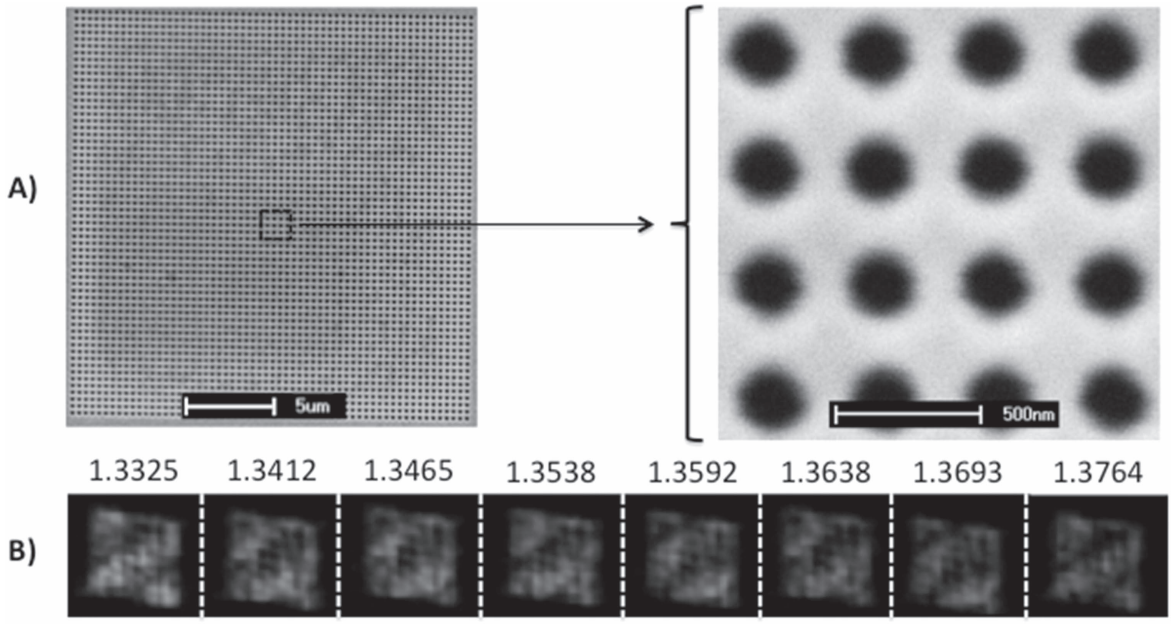

Figure 2. (A) SEM image of a nanohole array at different magnifications constructed by FIB in a 100 nm thick gold film supported on a glass slide. (B) CCD image samples for an array immersed in water (RI = 1.3325) and at aqueous glucose solutions (RI ranging from 1.3412–1.3764).

under all solutions. The highest possible flow was selected, ensuring system integrity and suppressing leakages. At this stage, a high flow is important to purge the system and remove the residues from previous solutions. The average transmitted light intensity was obtained from 50 images to compensate for laser fluctuations.

2.6. Biotests by intensity measurements

Initially, the sensor surface was cleaned with chloroform, acetone and distilled water in an ultrasonic bath for 10 min, and then assembled in an integrated system (figure 1). An aqueous solution (6.0 mM) of cysteamine was flowed over the arrays for 72 h (the time required for alkanethiol monolayer adsorption and organization). Afterwards, 5.0 mg ml^{-1} sulfo-NHS-biotin aqueous solution was flowed for 18 h. Subsequently, 0.5 mg ml^{-1} streptavidin in PBS solution was used for 4 h. Then, biotinylated antibody solution (50.0 μg ml^{-1} in PBS) was flowed for 4 h. Finally, HER2 antigen at a known concentration of 3.0 ng ml^{-1} (diluted in AS) was flowed on the substrate for 1 h. A flow of 0.04 ml h^{-1} (the lowest flow possible) was used for all the steps to ensure that the system was close to a resting condition during the immobilization step. Thus, the transport of biomolecules toward the surface is mainly dependent on diffusion. After each step, the system was purged with PBS (or AS after the antibody step to block non-specific sites) at a flow of 2.00 ml h^{-1} to remove the non-adsorbed molecules. After purging and resting, 50 array images were obtained for each modification step.

The PBS composition was 0.137 M NaCl, 0.00280 M KCl, 0.00810 M Na_2HPO_4, and 0.00150 M NaH_2PO_4; the pH was adjusted to 7.45 using 0.100 M NaOH and H_3PO_4 solutions, all diluted in Milli-Q water. The AS was composed of 0.1% (w/v) BSA (used as a blocker of non-specific sites and as a stabilizer), 0.1% (w/v) cold fish skin (blocker of non-specific sites) and 0.5% (v/v) triton X-100 (detergent used to decrease the surface tension and increase the solution 'wettability' on the substrate surface), all diluted in PBS.

3. Results and discussion

The SEM image of a nanohole array at different magnifications is shown in figure 2(A). The substrate used contained four similar nanohole arrays and they presented: 105 nm hole depth (metallic film thickness), *ca.* 557.6 μm^2 individual array area, *ca.* 400 nm periodicity (distance between the centers of the two neighbor holes regarding the *x*–*y* plane), and *ca.* 200 nm hole diameter.

Assuming light normal incidence on square arrays containing circular holes, the plasmonic transmission associated with the maximum wavelength can be predicted by equation (1),

$$\lambda_{máx} = \frac{a_0}{\sqrt{i^2 + j^2}} \sqrt{\frac{\varepsilon_d \varepsilon_m}{\varepsilon_d + \varepsilon_m}} \quad (1)$$

where λ_{max} is the maximum transmission wavelength, i and j are integers related to transmission order and a_0 is the array periodicity [22]. Arrays presenting these geometrical parameters provide a plasmonic transmission band around 633 nm ((2,0) plasmon mode). The (2,0) plasmon mode generates the most intense transmission band for the array [22]. Thus, the arrays were compatible for application in an experimental apparatus (as that shown in figure 1) based on the transmitted intensity measurements using a He/Ne laser. Optical investigation of the transmitted light through a nanohole array is a very efficient technique for real-time measurements and

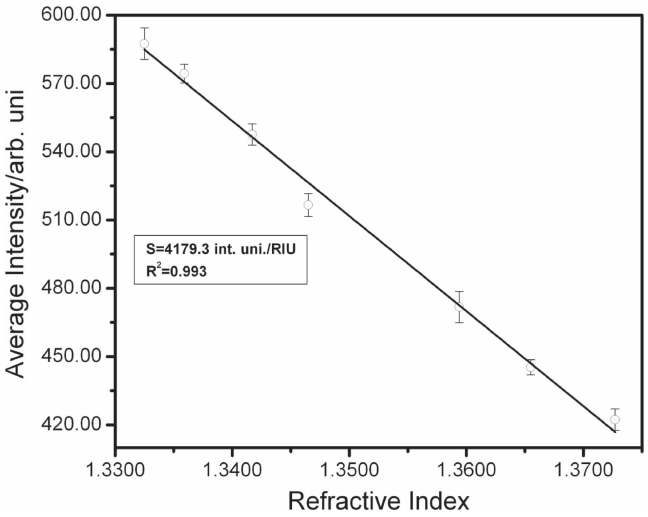

Figure 3. Average intensity of transmitted light (average from 50 images) through an array as a function of RI. Slope (S) is equivalent to array sensitivity, and R^2 relates to the linear adjustment of coefficient.

molecular characterization on a substrate surface. Using a compatible light source with the array transmission spectrum (taking into account the array geometric parameters—periodicity and hole diameter), it is possible to obtain suitable CCD images to monitor RI changes on the array surface.

To characterize the nanohole array sensitivity regarding RI variation, glucose solutions with different RIs, ranging from 1.3325 (Milli-Q water) to 1.3764 (more concentrated glucose solution) were flowed on the arrays. The CCD image samples for an array immersed in each sugar solution are shown in figure 2(B). Among the four arrays, those depicted here presented more homogeneous transmission images (figure 2(B)).

CCD images (figure 2(B)) have shown that the transmitted light intensity decreases as RI increases. This occurs because the increase on RI changes the conditions to excite SPs, leading to shifts on the plasmonic transmission bands for longer wavelengths [22]. So there is a decrease of the transmitted light intensity at a fixed wavelength of 633 nm (a laser was used).

CDD Images were obtained for another three arrays and the average value for the transmitted light intensity (average obtained from 50 images) was plotted as a function of RI to obtain array sensitivities. Figure 3 shows the sensitivity curve sample for an array. The curve slope (S) is defined as the sensitivity numerical value.

The highest array sensitivity value was 4179 int. uni./RIU (array in figure 2), and the average sensitivity was 4146 ± 39 int. uni./RIU, considering the four arrays in the substrate. The low standard deviation revealed suitable reproducibility concerning nanostructure performance. Small sensitivity differences possibly occur due to the presence of defects on the array structure obtained during FIB manufacturing, such as non-homogeneous periodicity, variable hole diameters, and local roughness.

It was evident that the proposed optical and electronic system was able to monitor the RI variation using intensity measurements. Another positive point is with regard to the R^2 values (between 0.970 and 0.993), showing a desired response with a fit to linear behavior. Thus, the sensor has excellent potential to be used on bioassays, mostly to detect cancer antigens that are often found at low concentrations in biological fluids.

In order to test the device viability concerning the biomolecule assessments, it was suggested that the sensor surface be prepared with antibodies against the HER2 antigen. For this, the sensor surface was initially modified using a cysteamine flow to form a spontaneous self-assembled monolayer of molecules via an interaction between thiol groups on a cysteamine and gold substrate [36]. Then, biotin molecules were immobilized on a pre-assembled alkanethiol monolayer by coupling primary amines onto the cysteamine network with carbonyl groups towards the sulfo-NHS-biotin molecule. Finally, the surface was coated with streptavidin molecules, which have a high affinity to biotin. These preliminary steps are illustrated in scheme 1.

Streptavidin surface presence (which contains other available sites for biotin) allowed immobilization of the biotinylated antibody. In sequence, the HER2 antigen was finally immobilized (direct detection mode). After each surface modification step, array images were acquired and samples are shown in figure 4(A). Looking at the images in figure 4(A), a decrease of transmitted light intensity was not so evident after surface modification. However, as shown in figure 4(B), the average value of transmitted light intensity through the array (the most sensitive array) clearly decreased when the antigen was bound to the antibody. This behavior was expected because the biomolecule presence changes the RI local on the SP region.

Figure 4 shows an intensity decrease of *ca.* 21 units after HER2 antigen immobilization. The results demonstrate that the system was able to monitor the HER2 antigen at a known concentration of 3 ng ml^{-1}, which is within the range found in the blood of healthy people. Furthermore, the signal-to-noise ratio obtained was *ca.* 3.0 (the standard deviation of the average intensity for HER2 immobilization was *ca.* 7 intensity units). This indicates that the device has high potential to detect the antigen, even at low concentrations, whereas the sandwich detection mode may also be employed to improve its performance. The assessed concentration was ten times less than that previously reported by our research group using an SPR biosensor based on a nanohole array operating with a spectral shift of the plasmonic transmission band [21], instead of the intensity measurements proposed here.

Further, the device developed here can be applied for HER2 assessment on human serum because the immunoassay uses monoclonal antibodies as biorecognition agents. Monoclonal antibodies are able to recognize a single epitope of the antigen, which significantly suppresses the possibility of non-target antigen recognition. Thus, the influence of other components on the sample matrix (blood is a very complex matrix) could not have much influence on the measures. In addition, our device operates with a microfluidic system,

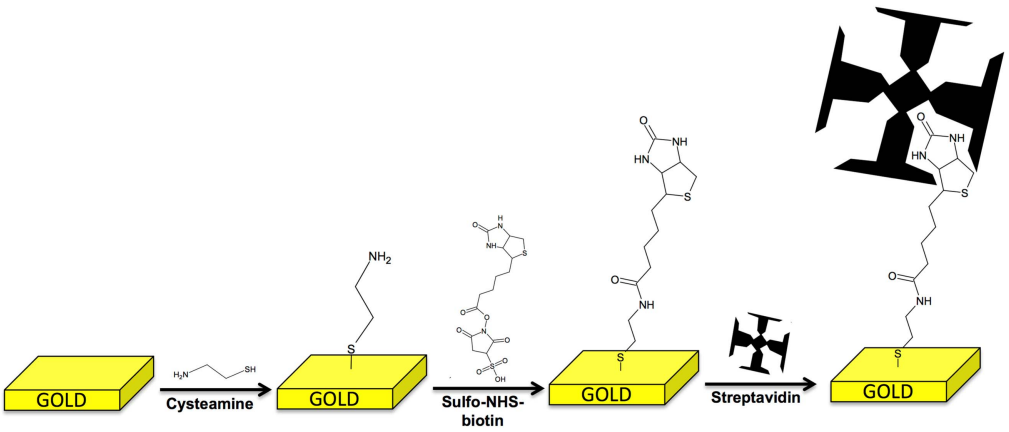

Scheme 1. Immobilization of streptavidin on gold surface.

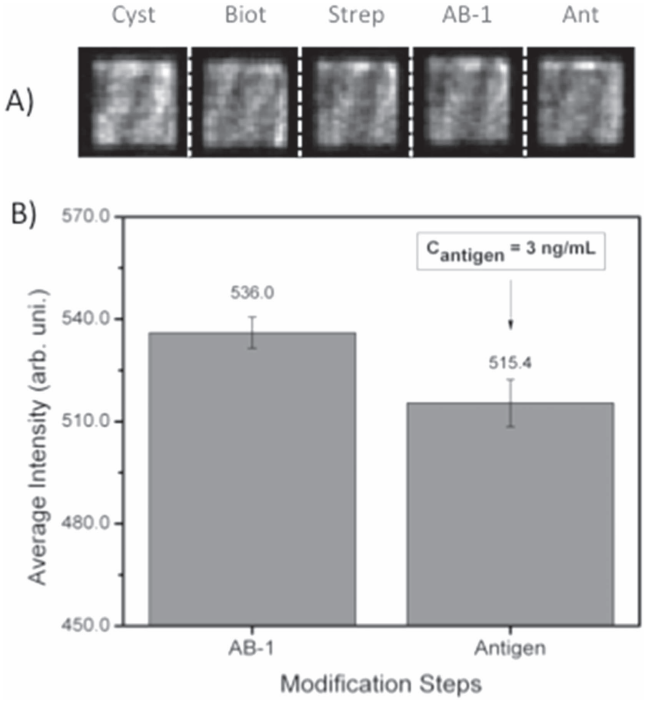

Figure 4. (A) CCD image samples of an array after each surface modification step; 'cyst' = cysteamine, 'biot' = biotin, 'strep' = -streptavidin, 'AB-1' = antibody, and 'ant' = antigen. (B) Average value of transmitted light intensity through an array on the last two modification steps. The average value for the steps was obtained from 50 images. The concentration of antigen ($C_{Antigen}$) flowed was 3 ng ml^{-1}.

which provides some advantages over the assay, such as decreased sample consumption and device miniaturization possibility.

4. Conclusions

The label-free biosensor based on a nanohole array proposed in this study showed 4146 int. uni./RIU average sensitivity using image acquisition to monitor transmitted light intensity through arrays. Thus, the device was able to monitor RI variation on a metallic surface. In addition, the proposed biosensor operates with a microfluidic system that allows the production of miniaturized sensors, compatible with lab-on-chip sensors (multiplexing sensors). We show that the biossensor enables us to detect the HER2 cancer antigen at 3.0 ng ml^{-1} known concentration, suggesting excellent applicability toward breast cancer diagnosis and prognosis. So the proposed device proved to have potential for use in bioassays, particularly in cancer marker assessments at low concentrations.

Acknowledgments

Johny P Monteiro and Sheila M Predabon thank CAPES and CNPq for the fellowships. We gratefully acknowledge Fundação Araucária (process no. 209/2014) for financial support. This work was also financially supported by CNPq (Brazil) by Inomat, National Institute (INCT) for Complex Functional Materials.

References

[1] Basil C F *et al* 2006 Common cancer biomarkers *Cancer Res.* **66** 2953–61
[2] Stefatic D, Riederer M, Balic M, Dandachi N, Stanzer S, Janesch B, Resel M, Ler D, Samonigg H and Bauernhofer T 2008 Optimization of diagnostic ELISA-Based tests for the detection of auto-antibodies against tumor antigens in human serum *Bosnian J. Basic Med. Sci.* **8** 245–50
[3] Vici P *et al* 2015 Triple positive breast cancer: a distinct subtype? *Cancer Treat. Rev.* **41** 69–76
[4] Freitas C S 2008 Extending knowledge on HER-family receptors for epidermal growth factor and their ligands to hematological malignancies *Revista Brasileira de Cancerologia* **54** 79–86
[5] Chamizo C, Rojo F and Madoz-Gúrpide J 2016 Determination of true ERBB2 gene amplification in breast cancer by quantitative PCR using a reference and a novel control gene *Appl. Immunohistochem. Mol. Morphol.* **24** 179–87
[6] Meenakshi A, Kumar R S and Kumar N S 2002 ELISA for quantitation of serum C-erbB-2 oncoprotein in breast cancer patients *J. Immunoassay Immunochem* **23** 293–305
[7] Krishnamurti U and Silverman J F 2014 HER2 in breast cancer: a review and update *Adv. Anat. Pathol.* **21** 100–7

[8] Tchrakian N, Flanagan L, Harford J, Gannon J M and Quinn C M 2016 New ASCO/CAP guideline recommendations for HER2 testing increase the proportion of reflex *in situ* hybridization tests and of HER2 positive breast cancers *Virchows Arch.* **468** 207–11
[9] Pauletti G, Dandekar S, Rong H, Ramos L, Peng H, Seshadri R and Slamon D J 2000 Assessment of methods for tissue-based detection of the her-2/neu alteration in human breast cancer: a direct comparison of fluorescence *in situ* hybridization and immunohistochemistry *J. Clin. Oncol.* **18** 3651–64
[10] Perez E A, Cortes J, Gonzalez-Angulo A M and Bartlett J M 2014 HER2 testing: current status and future directions *Cancer Treat. Rev.* **40** 276–84
[11] Wolff A C *et al* 2013 Recommendations for human epidermal growth factor receptor 2 testing in breast cancer: american society of clinical oncology/college of american pathologists clinical practice guideline update *J. Clin. Oncol.* **31** 3997–4013
[12] Qureshi A, Gurbuz Y and Niazi J H 2015 Label-free capacitance based aptasensor platform for the detection of HER2/ErbB2 cancer biomarker in serum *Sensors Actuators* B **220** 1145–51
[13] Arkan E, Saber R, Karimi Z and Shamsipur M 2015 A novel antibody-antigen based impedimetric immunosensor for low level detection of HER2 in serum samples of breast cancer patients via modification of a gold nanoparticles decorated multiwall carbon nanotube-ionic liquid electrode *Anal. Chim. Acta* **874** 66–74
[14] Saito M *et al* 2016 Serum HER2 as an adjunct to assess HER2 status for advanced gastric cancer: A prospective multicenter trial (SHERLOCK) *Acta Oncol.* **55** 309–17
[15] Oyama K *et al* 2015 *J. Gastroenterol.* **50** 41–5
[16] Zhu Y, Guo M, Zhang L, Wang L and Xu G 2016 Biomarker triplet NAMPT/VEGF/HER2 as a de novo detection panel for the diagnosis and prognosis of human breast cancer *Oncol. Rep.* **35** 454–62
[17] Gheybi E, Amani J, Salmanian A H, Mashayekhi F and Khodi S 2014 Designing a recombinant chimeric construct contain MUC1 and HER2 extracellular domain for prediagnostic breast cancer *Tumor. Biol.* **35** 11489–97
[18] Arikan O, Yyldyrym A, Ysbilen B, Canakci C, Atys G, Gurbuz C, Erol B, Ysman F K, Ozkanli S and Caskurlu T 2015 Clinical significance of serum and urinary HER2/neu protein levels in primary non-muscle invasive bladder cancer *Int. Braz. J. Urol.* **41** 1080–7
[19] Cooper M A 2006 Optical biosensors: where next and how soon? *Drug. Discovery Today* **11** 1061–7
[20] Hu D *et al* 2013 Comparison of surface plasmon resonance, resonant waveguide grating biosensing and enzyme linked immunosorbent assay (ELISA) in the evaluation of a dengue virus immunoassay *Biosensors* **3** 297–311
[21] Monteiro J P, Oliveira J H, Radovanovic E, Brolo A G and Girotto E M 2016 Microfluidic plasmonic biosensor for breast cancer antigen detection *Plasmonics* **11** 45–51
[22] Monteiro J P, Carneiro L B, Rahman M M, Brolo A G, Santos M J L, Ferreira J and Girotto E M 2013 Effect of periodicity on the performance of surface plasmon resonance sensors based on subwavelength nanohole arrays *Sensors Actuators,* B **178** 366–70
[23] Fano U 1941 The theory of anomalous diffraction gratings and of quasi-stationary waves on metallic surfaces (Sommerfeld's waves) *J. Opt. Soc. Am.* **31** 213–22
[24] Wood R W 1902 On a remarkable case of uneven distribution of light in a diffraction grating spectrum *Proc. Phys. Soc., London* **18** 269–75
[25] Otto A Z 1968 Excitation of nonradiative surface plasma waves in silver by the method of frustrated total reflection *Zeitschrift fur Physik* **216** 398–410
[26] Kretschmann E and Raether H 1968 Radiative decay of non radiative surface plasmons excited by light *Zeitschrift fur Naturforschung* A **A 23** 2135 –6
[27] Homola J 2008 Surface plasmon resonance sensors for detection of chemical and biological species *Chem. Rev.* **108** 462–93
[28] Brolo A G, Gordon R, Leathem B and Kavanagh K L 2004 Surface plasmon sensor based on the enhanced light transmission through arrays of nanoholes in gold films *Langmuir* **20** 4813–5
[29] Gordon R, Sinton D, Kavanagh K L and Brolo A G 2008 A new generation of sensors based on extraordinary optical transmission *Acc. Chem. Res.* **41** 1049–57
[30] De Leebeeck A, Kumar L K S, Lange V, Sinton D, Gordon R and Brolo A G 2007 On-chip surface-based detection with nanohole arrays *Anal. Chem.* **79** 4094–100
[31] Ebbesen T W, Lezec H J, Ghaemi H F, Thio T and Wolff P A 1998 Extraordinary optical transmission through sub-wavelength hole arrays *Nature* **391** 667–9
[32] Genet C and Ebbesen T W 2007 Light in tiny holes *Nature* **445** 39–46
[33] Ji J, O'Connell J G, Carter D J D and Larson D N 2008 High-throughput nanohole array based system to monitor multiple binding events in real time *Anal. Chem.* **80** 2491–8
[34] Lesuffleur A, Im H, Lindquist N C, Lim K S and Oh. S-H 2008 Plasmonic nanohole arrays for real-time multiplex biosensing *Proc. SPIE* **7035** 703504
[35] Yang J-C, Ji J, Hoglea J M and Larson D N 2009 Multiplexed plasmonic sensing based on small-dimension nanohole arrays and intensity interrogation *Biosens. Bioelectron.* **24** 2334–8
[36] Schmid A H, Stanca S E, Thakur M S, Thampi K R and Suri C R 2006 Site-directed antibody immobilization on gold substrate for surface plasmon resonance sensors *Sensors Actuators,* B **113** 297–303